APCC
APEC CLIMATE CENTER

TECHNICAL REPORT

APCC
APEC CLIMATE CENTER

PREFACE

It is our pleasure to present to you the APEC Climate Center (APCC)'s Technical Report 2011, which reports the core outcomes of our research activities from the past year.

Since 2005, APCC, as a hub of climate information in the Asia-Pacific region, has strived to share our analysis and prediction of abnormal climate and to apply this information to regional development. The center has established the largest Multi-Model Ensemble (MME) system for seasonal prediction through its international science network and has provided value-added products to various stakeholders. Recently, APCC has expanded its mandate to include enhancement of the capacity of APEC member economies information to respond effectively to climate change and variability through better application of climate.

To achieve its research and social objectives, in 2011, APCC made efforts to research improvements in its climate prediction performance from various angles and towards better understanding of climate variability and the reproducibility of the climate models for the relevant application of climate information to society. The following technical report provides more information about our research outcomes from 2011.

APCC will continue to improve the quality and accuracy of climate information, recognizing that the utility of this information is only as good as its quality. We would like to make the best use of our research results for the benefit of society and academia. We also welcome any feedback on this report or on our services.

My best and warmest regards to all of you.

Dr. Chin-Seung Chung
Director/APEC Climate Center

CONTENTS

APCC

TECHNICAL REPORT 2011-02

Assessment of the Long-Lead Probabilistic Prediction for the Asian Summer Monsoon Precipitation (1983-2010) Based on the APCC Multi-Model System and A Statistical Model

Dr. Soo-Jin Sohn

ABSTRACT

The performance of the probabilistic multi-model prediction (PMMP) system from the APEC Climate Center (APCC) in predicting the Asian summer monsoon (ASM) precipitation at a four-month lead (February initial condition) has been evaluated and compared with the corresponding prediction from a statistical model, based on hindcast data from 1983 to 2005 and real-time forecast data from 2006-2010. Particular attention was paid to the probabilistic prediction of precipitation in summers after the mature phase of El Niño and Southern Oscillation (ENSO) events. Taking into account the fact that the forecast skill of coupled models for the boreal spring and summer precipitation mainly comes from the models' ability to capture the ENSO teleconnection, we developed a statistical model based on a regression method using the preceding winter ENSO condition as a predictor. Although PMMP has limited skill for the ASM precipitation, it provides more consistent and stable skill than the statistical model. First, although the PMMP has a higher skill for both above- and below-normal categories during the real-time forecast period, the cross-validated statistical forecast has a higher skill during the 23-year hindcast, which indicates that the cross-validated statistical skill may be overestimated. Second, the PMMP is a better tool than the statistical model for capturing the atypical ENSO teleconnection that has affected the ASM precipitation during the recent decade and early 1990s. Third, the statistical model is more sensitive to the ENSO phase than the PMMP, thus it better predicts the ASM precipitation after the mature phase of La Niña.

1. INTRODUCTION

Long-range seasonal forecasts with up to a six-month lead, which are based on multi-model ensemble (MME) of coupled ocean-atmosphere-land models and used for the National Hydrological and Hydrometeorological Services within the Asia-Pacific Economic Cooperation (APEC), have been made operational by the APEC Climate Center (APCC) for some years [Lee et al., 2009]. The MME approach was designed for quantifying forecast uncertainties due to model formulations [Krishnamurti et al., 1999, 2000; Doblas-Reyes et al., 2000; Shukla et al., 2000; Palmer et al., 2000], and has been recognized as an effective way to improve dynamical weather and climate forecasts. The use of the MME technique for predicting seasonal climate anomalies and quantifying the associated uncertainties has become commonplace in major operational centers [Palmer et al., 2004; NOAA Climate Test Bed, 2006; Lee et al., 2009].

Most previous studies using historical retrospective forecasts (usually referred to as hindcasts; shown by Graham et al. [2005]; Palmer et al. [2004]; Wang et al. [2009]) for long-lead coupled model prediction systems have focused on deterministic predictions [Wang et al., 2008; Liang et al., 2009; Lee et al., 2010, 2011b]. However, climate forecasts have degrees of uncertainty that can be conveyed in terms of probabilities. Owing to their ability to quantify and communicate uncertainties, probabilistic forecasts provide more useful information and better aid the decision making of end users than do deterministic forecasts [Murphy, 1977; Krzysztofowicz, 1983; Palmer et al., 2004; Richardson, 2006; Alessandri et al., 2011]. For seasonal forecasts based on climate models, the level of uncertainty can be derived from an ensemble of model predictions [Murphy and Winkler, 1987; Tracton and Kalnay, 1993; Wilks, 1995]. By applying the same concept to multi-model predictions, a probabilistic seasonal prediction system based on MME outputs has also been developed [Min et al., 2009, 2011].

At present, state-of-the-art coupled models have shown reasonably good skills for ENSO prediction up to 6 months and beyond [Jin et al., 2008; Wang et al., 2009]. However, prediction of the summer mean precipitation over the Asian summer monsoon (ASM) region, even for a lead time as short as one-month, has proven to be difficult [Wang et al., 2007, 2008, 2009; Kug et al., 2008; Lee et al., 2010, 2011b]. That said, recent studies suggest that model prediction skill for the summer precipitation tends to increase after the mature phase of El Niño and Southern Oscillation (ENSO) has passed, particularly over East Asia and the Western North Pacific (WNP) monsoon region [Wang et al., 2009; Liang et al., 2009; Chowdary et al., 2010; Lee et al., 2011a, 2011b]. Thus, in principle, accounting for ENSO together with its lagged impact on the ASM precipitation can aid in statistical prediction modeling of the ASM region.

Numerical models that represent the dynamics of the atmosphere, ocean, and land should be able to give better seasonal forecasts than purely statistical approaches, because of their ability to handle a wide range of linear and nonlinear interactions and their potential resilience against a changing climate [van Oldenborgh et al., 2005]. Nonetheless, statistical methods have been widely used in seasonal predictions, and

oftentimes they give prediction skills comparable to those based on dynamical models [Anderson et al., 1999; Barnston et al., 1999; van Oldenborgh et al., 2005], although model biases remain a major source of errors [Latif et al., 2001; Palmer et al., 2004], particularly for the ASM region [Kang et al., 2004]. One advantage of the statistical forecast approach is that knowledge obtained from forecast data analysis can be easily applied. However, the statistical approach to long-lead prediction requires careful use of conventional statistical modeling techniques, especially due to the relatively short periods of record of observed databases and the existence of long-term change in the climate system. It is therefore worthwhile to investigate the extent to which a physically based statistical model can outperform the ASM precipitation predictions from dynamical models.

With the above as motivations, this study seeks to diagnose the long-lead probabilistic multi-model prediction (PMMP) assembled from four coupled models initiated on February 1st for the real-time forecast period of 2006 to 2010 as well as for the hindcast period of 1983 to 2005, with a focus on the prediction of ASM precipitation after the mature phase of ENSO. The rest of this paper is organized as follows. Section 2 describes the coupled models and hindcasts being considered, as well as the observational data and methodology used in the present study. Verifications of the PMMP of ASM precipitation are conducted in subsection 3.1 using reliability diagrams, relative operating characteristic (ROC) curves and the ROC score for the hindcast period. Verifications of the regression-based statistical model during the same period are shown in subsection 3.2. Subsection 3.3 compares the real-time forecast skill (2006-2010) of the dynamical and statistical models for the ASM precipitation. A summary and conclusions are given in sections 4 and 5.

2. DATA AND METHODOLOGY

2.1 The APCC PMMP system

APCC has conducted six-month-lead seasonal climate prediction using ocean-atmosphere-land coupled models since 2008, with the results issued four times a year. Table 1 describes the four coupled models component to the 6-month seasonal prediction system. This study evaluates the predictions covering the March-April-May (MAM) and June-July-August (JJA) seasons, which are based on coupled models initiated in February. All coupled model hindcast experiments cover the 23-year period of 1983 to 2005, and real-time forecasts for the five-year period of 2006 to 2010 are also considered. PMMP is constructed based on an uncalibrated multi-model approach, with model weights inversely proportional to the forecast probability errors associated with the model sampling errors (shown by Min et al. [2009]), and a non-parametric empirical ranking method for estimating tercile-based categorical probabilities.

Table 1 Acronyms and description of models used in this study.

Institute	Model	AGCM	Resolution	OGCM	Resolution	Ens. member	Reference
APCC	CCSM3[1]	CAM3[2]	T85 L26	POP1.3[3]	g x lv3 L40	5	Jeong et al. [2008]
NCEP	CFS	GFS[4]	T62 L64	MOM3[5]	1/3°lat x 5/8°lon L27	15	Saha et al. [2006]
FRCGC[6]	SINTEX-F[7]	ECHAM4[8]	T106 L19	OPA[9]8.2	2°cos(lat) x 2°lon L31	9	Luo et al. [2005]
SNU	SNU	SNU	T42 L21	MOM2.2	1/3°lat x 1°lon L32	6	Ham and Kang [2010]

1) Community Climate System, version 3.0
2) Community Atmospheric Model, version 3.0
3) Prarellel Ocean Progam
4) Global Forecast System [*Moorthi et al.*, 2001]
5) GFDL Modular Ocean Model version 3 [*Pacanowski and Griffies*, 1998]
6) Frontier Research Center for Global Change
7) Scale INTeraction Experiment-FRCGC
8) The fourth-generation atmospheric general circulation model of the European Centre for Medium-Range Weather Forecasts –Deutsches Klimarechenzentrum: Hamburg
9) Océan PArallélisé [*Roeckner et al.*, 1996]

2.2 Statistical model

Motivated by the fact that the ASM precipitation tends to be more predictable after the mature phase of ENSO, I developed a regression-based statistical model with the ENSO condition in the preceding boreal winter as the predictor. The conditional probability, P(B|A) is defined as the transfer function of the predictand and the predictor. This conditional probability is the probability of some event B, given the occurrence of some other event A; as applied in the present study, A is the preceding winter ENSO condition (defined as the value of the Niño 3.4 index; see section 2.3) and B represents the impact of an ENSO event on the ASM rainfall. In other words, the probabilistic composites are formulated based on the probabilities of the ASM rainfall for a given state of the ENSO, such as El Niño (total of 7 years), La Niña (8 years), and the neutral state (8 years), during the training period. The thresholds of tercile for three equiprobable categorical probabilities, i.e., above normal (AN), near normal (NN), or below normal (BN), are determined based on the empirical probability density function (PDF) with respect to the climatology of the whole training period (i.e., 23 year variability). With these two boundaries, the tercile-based categorical probabilities of the composites are obtained by counting the number of specific years in each category for a particular ENSO state (e.g. 7 years for El Niño).

The statistical forecast model is constructed as follows. First, the probability of the Niño 3.4 index (PA) is estimated as a portion of the climatological PDF of the indices during the training or cross-validated hindcast period [Michaelsen, 1987]. The hindcast period index is employed to prevent skill score overestimation; that is, the calculation of the climatological PDF is repeatedly applied to data from which one year is excluded and the estimation of probability for the Niño 3.4 index is made for the excluded year. By repeating this process for all years, we obtain a full set of probabilities for the Niño index that can be applied to the statistical forecast model.

The probability PB of the predictand B is computed as follows:

$$P_B(E_j) = \sum_{i=1}^{3} P_{B|A}(E_j) P_A(E_i)$$

where PA is the probability of the predictor A, and E_j and E_i are the *j* and *i* events, respectively [in this case the AN, NN, or BN categories]. For this statistical model, the probabilistic forecast field for the ASM precipitation is then calculated by combining the probability of the status of ENSO (P_A) with the associated composite maps ($P_{B|A}$). Finally, in order to compare the statistical and dynamical forecasts, we have produced a cross-validated statistical forecast for the 23 year period of 1983 to 2005, and for the independent forecast covering 2006 to 2010 (with 1983 to 2005 being the training period).

2.3 Observational datasets

The observed precipitation data used in this study are those of the Climate Anomaly Monitoring System (CAMS) and Outgoing Longwave Radiation (OLR) Precipitation Index (OPI) (CAMS OPI; Janowiak and Xie, [1999]). CAMS OPI is a precipitation analysis which merges observations from rain gauges with estimates from satellites to produce monthly mean global precipitation in quasi real time. CAMS OPI has been found to be reliable for monitoring large-scale precipitation variation over the East Asian sector [Sohn et al., 2011]. This rainfall dataset is used to assess the model forecasting skills and form the probabilistic composite maps for ASM precipitation based on the Niño 3.4 index. All data used in this study are interpolated onto a 2.5°×2.5° grid.

The ENSO condition is defined using the Niño 3.4 index[10], which is calculated from the optimum interpolation (OI) of sea surface temperature (SST) data [Reynolds et al., 2002]. Periods during which the standardized value of the DJF Niño 3.4 index is greater than 0.5 are identified as an El Niño event; they are the winters of 1982/83, 1986/87, 1987/88, 1991/92, 1994/95, 1997/98, 2002/03 and 2009/10. The boreal winters of 1983/84, 1984/85, 1985/86, 1988/89, 1995/96, 1998/99, 1999/2000, 2000/2001, 2005/06, 2007/08 and 2008/09, when the Niño 3.4 index is less than -0.5, are identified as La Niña events.

10) Niño 3 is correlated at 0.98 to the tropical Pacific SST's PC1 and does not have the problems of the Niño 3.4 index, which captures signals of both EOF 1 and EOF2 types of ENSOs [*Ashok et al., 2007*]. A comparison of lagged impacts based on these indices is a subject of further research.

2.4 Forecast quality assessments

The measures used for assessing deterministic MME forecast skill include the temporal correlation coefficient (TCC) skill and the pattern correlation coefficient (PCC) skill. The PCC skill is a measure of the spatial correlation coefficients between two datasets over an area of interest [*Wang et al., 2004*].

To evaluate the probability forecast skills, we use reliability (attributes) diagrams [*Murphy*, 1973; *Murphy and Winkler*, 1977; *Wilks*, 1995; *Jolliffe and Stephenson*, 2003; *Atger*, 2003, 2004], the relative operating characteristic (ROC; *Swets* [1973]; *Mason* [1982]; *Wilks* [1995]; *Mason and Graham* [1999]; *Richardson* [2000]; *Zhu et al.* [2002]) curves and the Area under the ROC curve (AROC, ROC score or ROCS; *Green and Swets* [1966]), following the recommendations of the World Meteorological Organization (WMO) Standardized Verification System for Long–Range Forecasts (SVS–LRF; *WMO* [2002]; further details are given by *Min et al.* [2009]). To assess the skill of the forecasts compared to climatological forecasts in each category, we use the Brier skill score (BSS; *Murphy* [1973], *Stanstki et al.* [1989]; detailed descriptions are given by *Wilks* [1995]). Wang et al. [2009] demonstrated that two measures of probabilistic forecast, the BSS and ROCS, have forecast skills with similar spatial distributions that are also similar to the spatial pattern of the TCC skill.

The reliability diagram displays the relative frequency of an observed event against the forecast probability of the event for the bins into which the forecasts are grouped. The diagonal connecting the point (0, 0) and (1, 1) represents the perfect forecast, i.e. for resolution and reliability. The line with a relative frequency value of 0.333, the “no resolution” line, corresponds to the performance of random forecasts. The median of the angle between these two lines, the line where reliability is equal to resolution, represents the performance of the climatological forecast. The closer the curve is to the diagonal, the higher the forecast skill.

The ROC is the signal detection curve obtained by plotting a graph of hit rate against false alarm rate over a range of different probability thresholds. Its curve travels from the bottom left to the top left of the diagram, then across to the top right of the diagram. A diagonal line indicates no skill, i.e. the hit rate and false-alarm

rate are equal. The ROCS is a way to quantify the ROC by calculating the area beneath the ROC curve [*Green and Swets*, 1966]. The ROCS is equal to 1 (unit area) for a perfect forecast and 0.5 for a forecast that corresponds to the climatological forecast. If the ROCS is less than 0.5 (i.e. the same as a no-skill forecast), then the model is less skillful than a random or constant forecast.

The statistical significance of the obtained verification scores has been assessed using the Monte Carlo approach [*Stephenson and Doblas-Reyes*, 2000]. We have randomly scrambled the forecast fields 500 times in the time domain.

3. RESULTS

3.1 Evaluation of PMMP

To begin with, we examine the TCC skill of the MME comprising the four coupled models for predicting the MAM and JJA precipitation, all of which have a February initial condition, for the hindcast period of 1983 to 2005. Here, the MME average was computed based on a simple composite method (i.e. one with equal weights for all models; see also *Sohn et al*. [2011a]).

Figure 1 shows the TCC for the MAM and JJA precipitation predictions based on the hindcast dataset. It can be seen that the deterministic MME gives much better skill in MAM than in the JJA season, especially over the eastern Indian Ocean to the Western Pacific Ocean, Central Asia, some parts of East Asia including Korea, Japan, and the central to eastern portion of northern China adjoining Mongolia. We have also compared the TCC skills of the MME predictions based on all years (Figures 1a and 1b, total of 23 years), those after the mature phase of ENSO (Figures 1c and 1d, total of 15 years; see also section 2.3), and the remaining normal seasons (8 years). The similarity between the results based on all years and those based only on those years after mature ENSO events suggests that the coupled models' skill mainly comes from their ability to capture the impact of ENSO. For the MAM precipitation, the TCC skill of the coupled models over the western Pacific after

the ENSO peak is even higher than that based on the whole hindcast record. The lagged impact of ENSO on ASM rainfall still remained in the model environments through the subsequent JJA season, albeit with lower skill over most continental Asian locations. On the other hand, for normal years, it is found that the one-month lead MAM forecast skill is no greater than that of the four-month lead JJA forecast skill (shown in Figure 2).

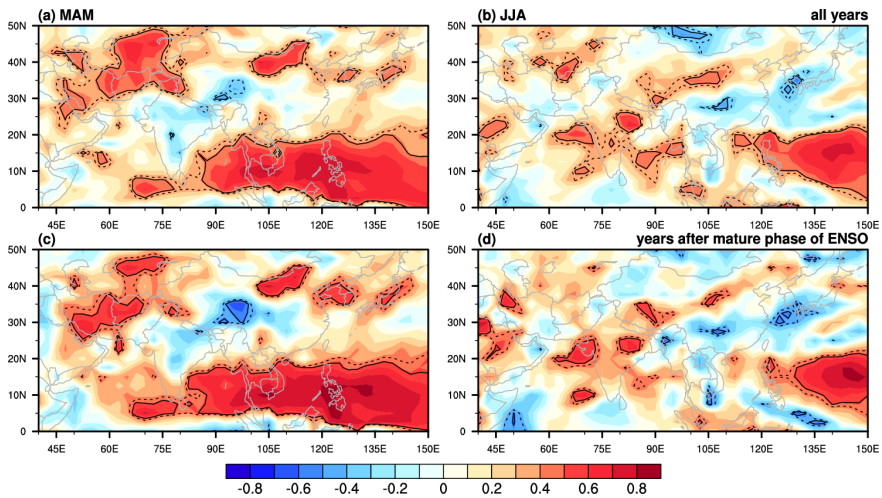

Figure 1 TCC between observations and the MME prediction for (a, c) MAM and (b, d) JJA precipitation during (a, b) all years and (c, d) years after mature phase of ENSO. Dashed and solid lines denote the threshold values for the 90% and 95% significant levels, respectively.

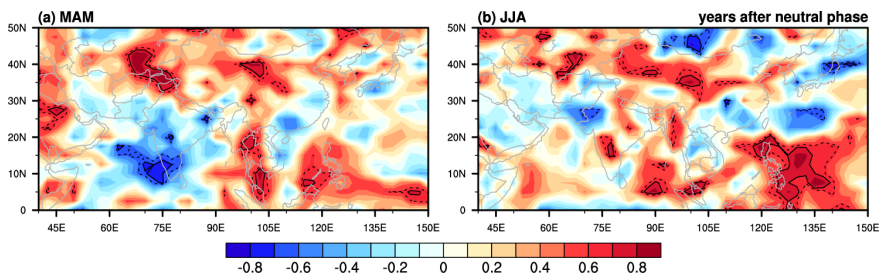

Figure 2 TCC between observations and the MME prediction for (a) MAM and (b) JJA precipitation during years after the neutral phase. Dashed and solid lines denote the threshold values for the 90% and 95% significant levels, respectively.

Figure 3 shows the general performances of PMMP for seasonal precipitation in terms of the spatial distribution of ROCS. The majority of areas with significant skill for MAM prediction are located in the eastern Indian Ocean to the Western Pacific Ocean, Central Asia, and some parts of East Asia for the AN category (Figure 3a). Similarly, the skill for the BN category was significant for most of the abovementioned locations as well as the western Indian Ocean. Notice that the ROCS plots for the AN and BN categories display patterns very similar to the TCC score of the MAM deterministic forecast (see Figure 1a). For JJA, the skill of the probabilistic MME decreases drastically, especially over continental Asia. Overall, the above analysis reveals that the coupled model MME can predict the MAM mean precipitation over some parts of Asia with high fidelity, but over most ASM locations, the MME has difficulty predicting the JJA mean rainfall.

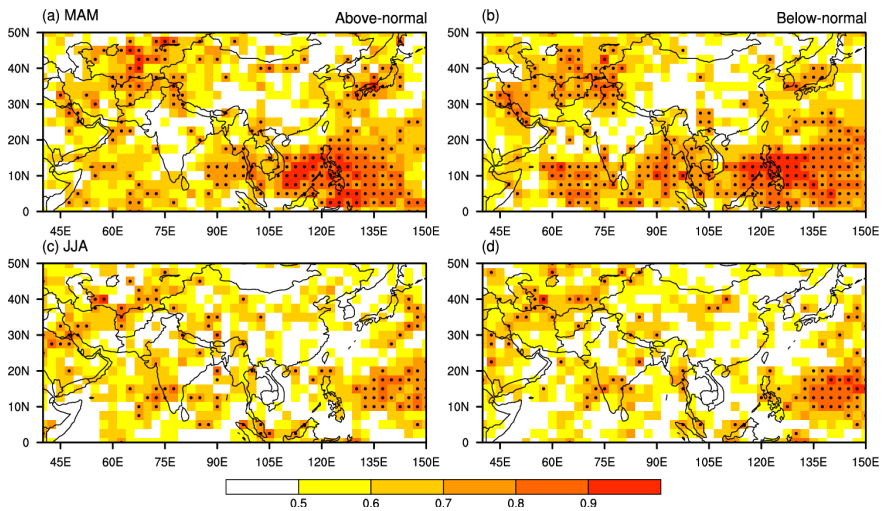

Figure 3 ROCS of PMMP for (a, b) MAM and (c, d) JJA precipitation for (a, c) the AN and (b, d) BN categories. The black dots indicate grid points for which the ROCS is significant at the 95% confidence level, as determined by the Monte Carlo test with 500 random trials.

The regionally aggregated reliability diagrams for PMMP with the corresponding frequency histograms, for the Asia monsoon region (0-50°N, 40-150°E) and East Asia (20-50°N, 90-150°E), are shown in Figure 4. PMMP generally follows the typical bias feature, based on the diagonal line, which indicates an underestimation (i.e. above the diagonal line) in low probability and overestimation (below the diagonal line) in high probability compared to the observed relative frequency (except the AN category for MAM over the ASM region). For the MAM precipitation, deviation of the PMMP curve from the diagonal is quite small. For the AN and the BN categories, MAM precipitation forecasts outperform climatology (i.e. reliability is equal to resolution) for the Asia monsoon region and are definitively more skillful than random forecasts (i.e. no resolution) for East Asia. The skill of PMMP for the JJA precipitation is lower than that for MAM; however, note that the JJA precipitation forecasts are still more skillful than random guessing for the Asia monsoon region for both categories. The curves of both categories for East Asian JJA precipitation are divergent from each other. The AN curve even falls beneath the no-resolution line for high probability, exhibiting minimal resolution. To quantify the bias of PMMP, we have also evaluated the BSS value for the each category. The regionally aggregated BSS values of PMMP are shown in the top-left corner of the plots. For the AN category, the MAM and JJA precipitation forecasts are more skillful than those for the BN category for both regions (i.e. the positive value of the BSS indicates that PMMP outperforms climatological forecasts in the AN category). Also, the analyses show that for both regions, the predictions become less reliable as the forecast lead time increases.

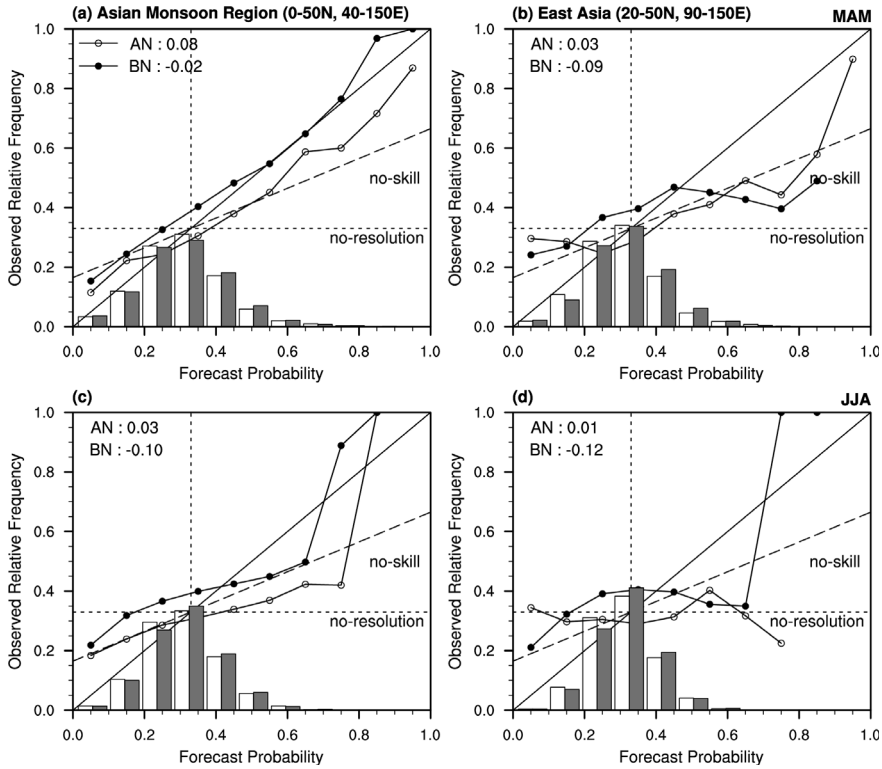

Figure 4 Reliability diagram and frequency histogram for PMMP for (a, b) MAM and (c, d) JJA precipitation for (a, c) the Asian monsoon region (0-50°N, 40-150°E) and (b, d) East Asia (20-50°N, 90-150°E). White (grey) bars and open (closed) circles indicate relative frequency and reliability for the AN (BN) category, respectively. The area-averaged values of the BSS score over each region are provided in the upper left of each panel.

Regionally aggregated ROC curves and their ROCS are also used to assess the performance of PMMP during the hindcast period (results are shown in Figure 5). The ROC curves are found to be consistent with the reliability diagrams (see Figure 4). For the MAM forecast, the curve is farther away from the diagonal to the left and upward directions, compared to its JJA counterpart. The regionally aggregated ROC scores for the MAM forecast are much higher than for the JJA forecast and are also above 0.5 (i.e. the value for no-skill forecast), thus the forecast could be considered to be skillful. In contrast, the ROC scores for the JJA forecast for the Asia monsoon region and East Asia give low skills of 0.55 (0.55) and 0.51 (0.51) for the AN (BN) categories, respectively. For other regions, the results are presented in Figure 6.

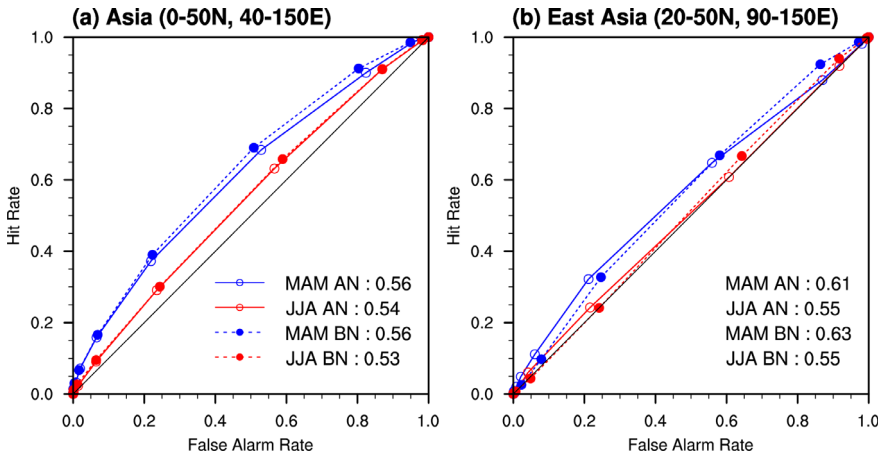

Figure 5 ROC curves for PMMP precipitation for (a) the Asian monsoon region (0-50°N, 40-150°E) and (b) East Asia (20-50°N, 90-150°E). Blue (red) lines and open (closed) circles indicate the False Alarm Rate to Hit Rate for MAM (JJA) precipitation and the AN (BN) category, respectively. The area-averaged values of ROC score over each region are provided in the bottom left of each panel.

In summary, we have examined the forecast skills of the deterministic MME prediction and PMMP for ASM precipitation. Results reveal that coupled models are able to well predict the Asian monsoon rainfall variability during the MAM season, but not for the JJA season. It is noticed that the forecast skills mainly come from the coupled models' ability to capture climate anomalies after the mature phase of ENSO. On the other hand, the forecasts exhibit very low skills after normal winters in both the MAM and JJA seasons.

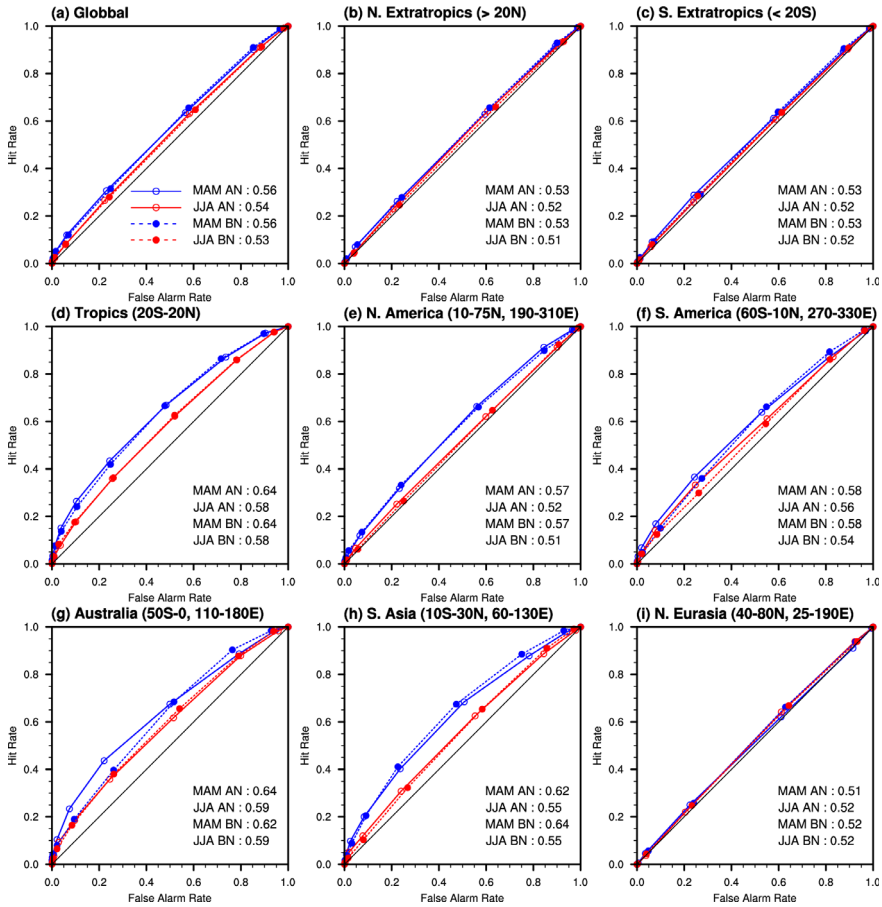

Figure 6 ROC curves for PMMP precipitation for the various regions.

3.2 Development of the statistical model using its climate contributor

To find out the global impact of ENSO after its peak phase in boreal winter, the temporal correlation coefficient between the DJF value of the Niño 3.4 index and precipitation in the following JJA season has been calculated. Results are shown in Figure 7. Positive correlation is found over Western to Central Asia, Northeast Asia adjoining the Northwest Pacific, and the equatorial central and eastern Pacific adjacent to Latin America. Negative signals are located in the tropical western Pacific, in the South Pacific trailing the South Pacific convergence zone (SPCZ), and over

most of Brazil. It is noteworthy that strong signals are found over the western Pacific, consistent with previous studies showing that the East Asian summer monsoon variations are linked to decaying El Niño or La Niña [Wang et al., 2004, 2008, 2009; Lee et al., 2011a, 2011b; Chowdary et al., 2010]. Results for other seasons are presented in Figure 8.

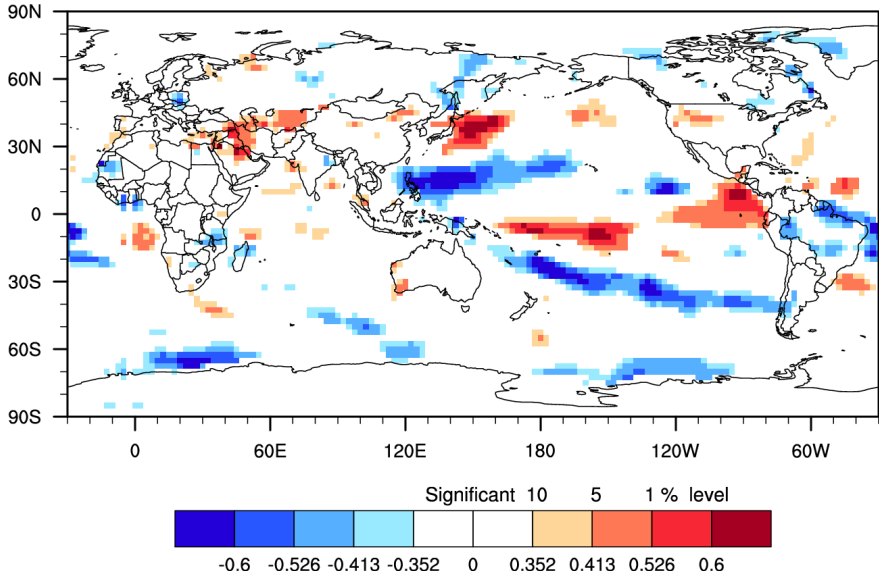

Figure 7 TCC between Nino 3.4 index for the preceding DJF and the mean precipitation in the following JJA season. Values with absolute magnitudes of 0.526, 0.413 and 0.352 represent the 99, 95 and 90 % significant levels, respectively.

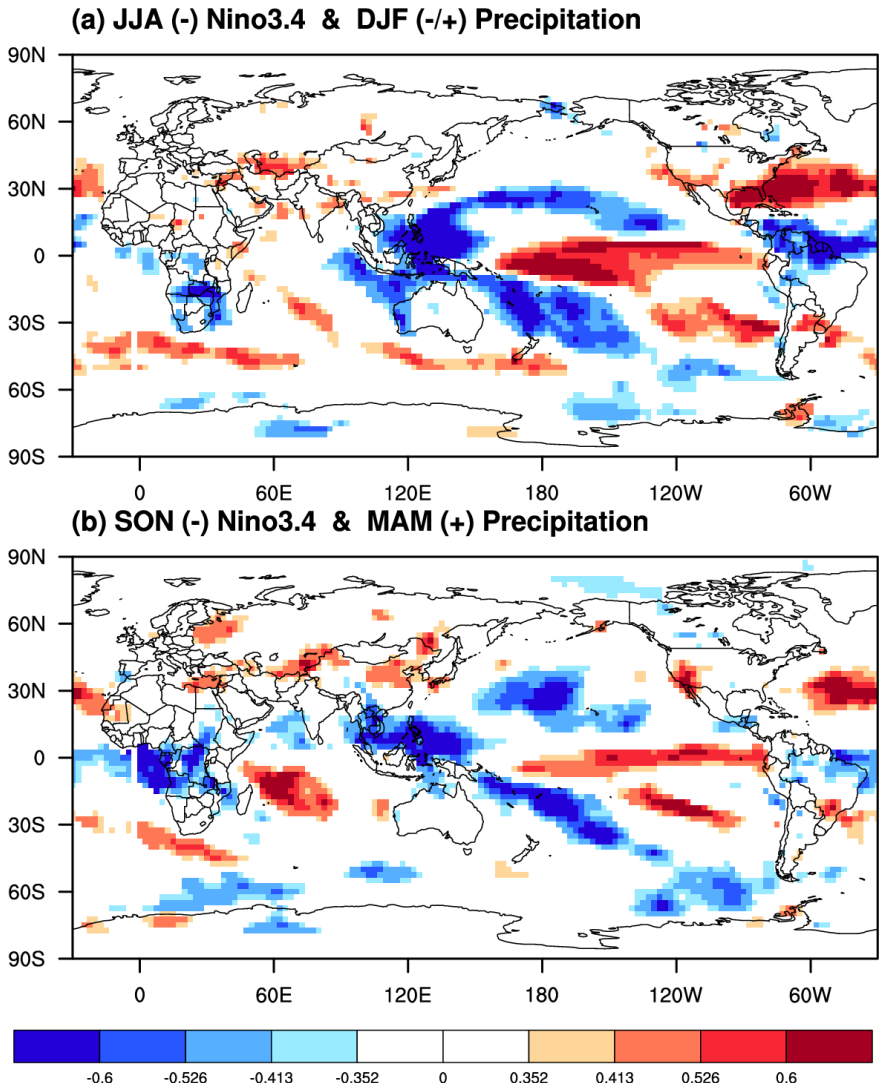

Figure 8 TCC between the preceding Nino 3.4 index and the following seasonal mean precipitation.

To depict the precipitation patterns related to the ENSO condition in the previous winter, probabilistic composites are computed by ranking JJA mean precipitation for the years after which the preceding DJF Niño 3.4 index is -0.5 (+0.5) standard deviation below (above) average (see also section 2). Figure 9 shows the probabilistic composites of JJA mean precipitation over the ASM region for the AN and BN categories,

after the mature phase of ENSO during the training period. The probabilistic composites of ASM precipitation show asymmetries in their spatial patterns, and the strengths of their associated probabilities between the lagged effects of the preceding El Niño and La Niña conditions are in opposite phases, e. g. warming and cooling, across the tropical Pacific Ocean from each other. The regional distribution of probabilistic composites associated with El Niño for the AN category mainly shows wetter-than-normal conditions over the Indian Ocean, Central Asia, central China, and the northwest Pacific covering Korea and the Japanese archipelago. The strongest signals for the BN category are found to be located more eastward than those of the AN category, which indicates drier-than-normal conditions along coastal East Asia spanning Korea, Taiwan and southern China, as well as over eastern India and the tropical Western Pacific. On the other hand, La Niña effects drier-than-normal conditions over many Asian monsoon regions. There is no significant signal for the AN category except over the Philippines and the adjoining tropical Western Pacific.

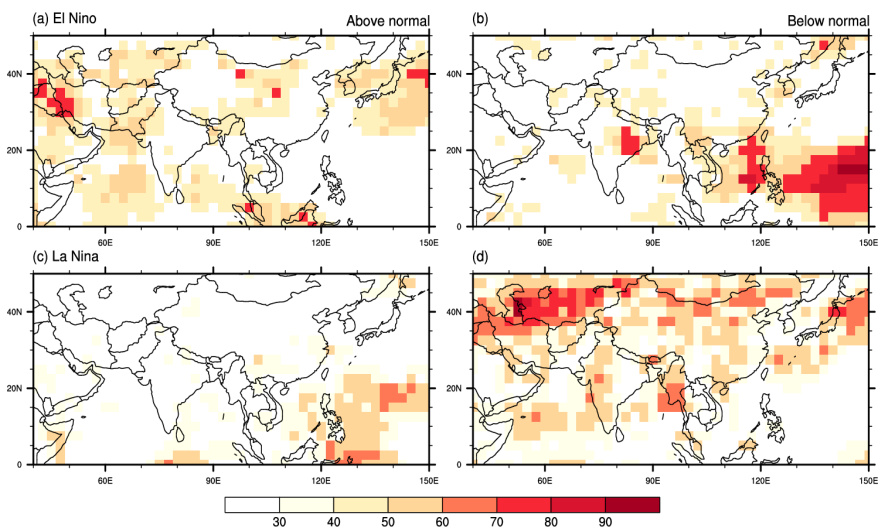

Figure 9 Conditional probabilistic composites of the JJA seasonal mean precipitation after the mature phase of ENSO for (a, b) El Niño and (c, d) La Niña years for the (a, c) AN and (b, d) BN categories.

The combined one is based on three category probabilities, where one of the categories dominates with corresponding color and the PDF significantly differs from

the climatological one at the 95% significant level, as determined by Pearson's chi-square (χ^2) test (see *Min et al.* [2009] for more details; Figure 10). In summary, the lagged impact of El Niño on ASM precipitation is characterized by more local response which simultaneously indicates above normal probability over the western Indian Ocean, Central Asia, the western-to-central part of northern China, and Northeast Asia, and below normal probabilities from the western tropical Pacific extending into Indochina. On the other hand, it is more likely for continental Asia to experience drier-than-normal conditions after the mature phase of La Niña. Results for the SON and DJF seasons are presented in Figures 11 and 12.

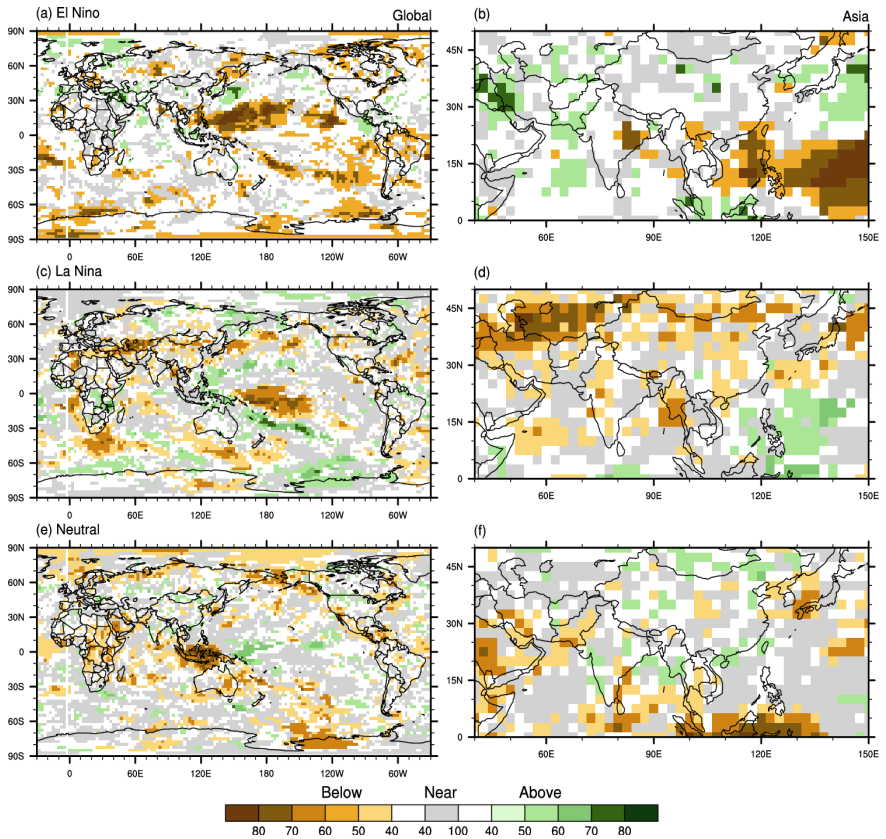

Figure 10 Combined maps of conditional probabilistic composites for the JJA seasonal mean precipitation over (a, c, e) the globe and (b, d, f) the Asia monsoon region after the mature phase of ENSO for (a, b) El Niño, (c, d) La Niña, and (e, f) neutral years. The maps show regions where either the AN, NN or BN category is dominant, based on Peason's chi-square (χ^2) test.

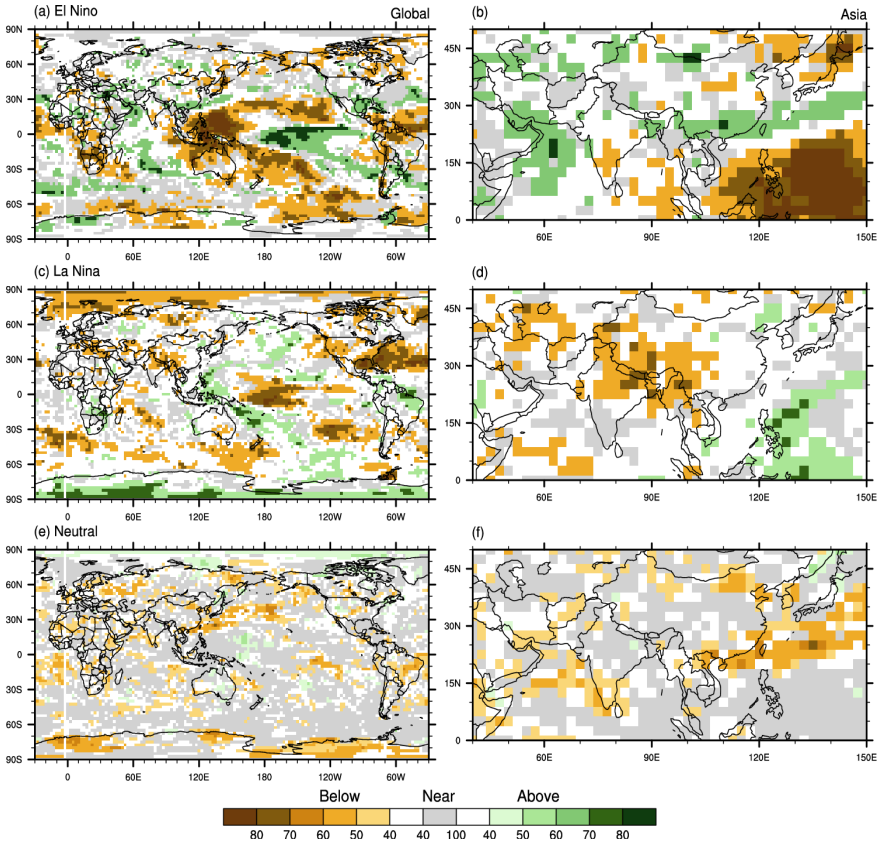

Figure 11. Same as Figure 10 but for the SON seasonal mean precipitation.

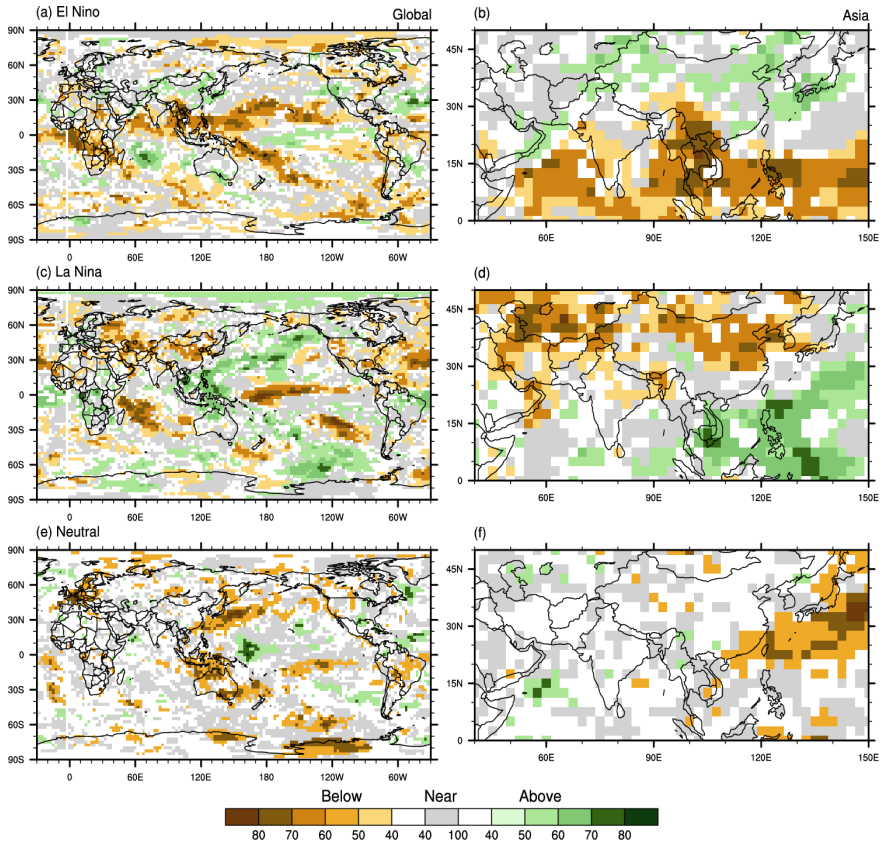

Figure 12 Same as Figure 10 but for the DJF seasonal mean precipitation.

3.3 Evaluation of the statistical prediction model

A cross-validated statistical forecast for the ASM precipitation is gained by projecting the status of the preceding ENSO onto the composite map produced in a cross-validated mode (i.e. the precipitation field for the forecast year is not reflected in the composite). It is interesting to note that the statistical model has better skill than the dynamical model, especially over Northeast Asia and some parts of Southern Asia, during the cross-validation period (Figure 13). Due to the design of the statistical model, the spatial distributions of the forecast skills for the AN and BN categories are similar to that of the observed probability composites for El Niño and La Niña (Figures 9 and 10).

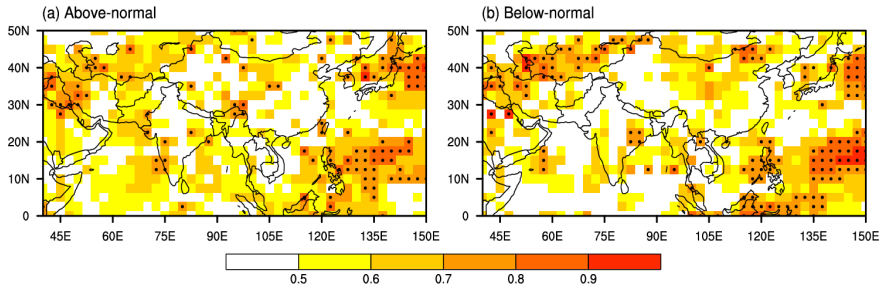

Figure 13 ROCS of the statistical model for the JJA mean precipitation for the (a) AN and (b) BN categories.

The performance of the statistical model is also assessed using regionally aggregated reliability diagrams and ROC curves for the cross-validated period. In comparison with PMMP, there are three interesting features. First, the statistical prediction also has the typical bias characterized by underestimation in the low probability and overestimation in the high probability, similar to PMMP (Figure 14). Second, the statistical model has better reliability and resolution than PMMP for both the AN and BN categories. In terms of ROCS, the statistical model is better than PMMP, especially over the East Asian region where PMMP has marginal skill close to 0.5 (shown in Figure 15). Third, the statistical model performs better for AN than for BN events in Asian and East Asian locations, while PMMP has similar skill for the two categories. For other regions, the results are presented in Figure 16. The results for the SON and DJF seasons are presented in Figures 17 and 18.

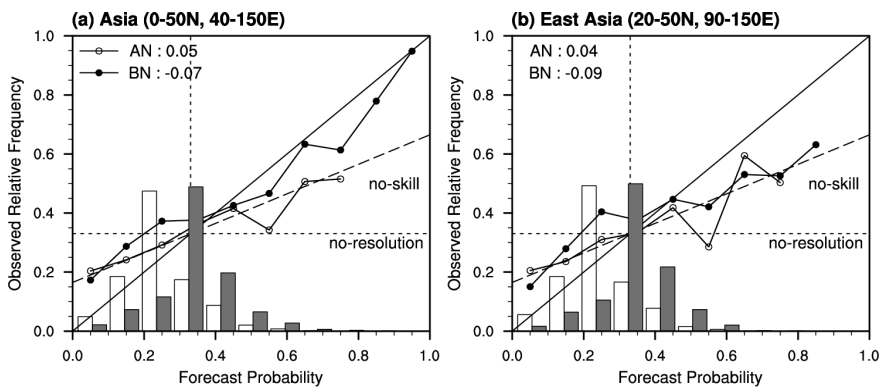

Figure 14 Reliability diagram and frequency histogram for the statistical model for the JJA mean precipitation over (a) the Asian monsoon region and (b) East Asia.

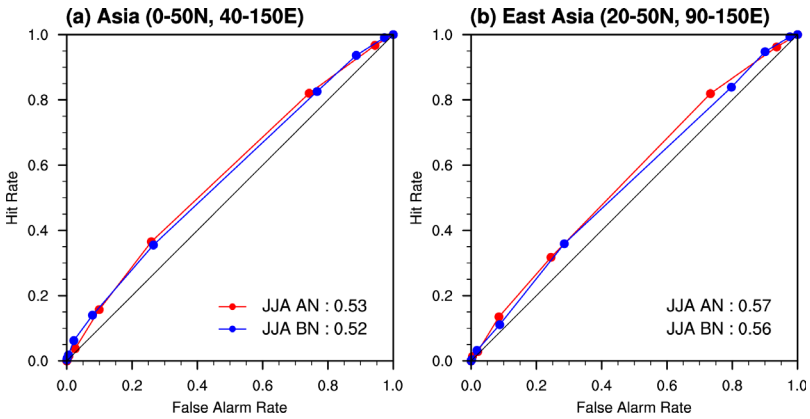

Figure 15 ROC curves for the statistical model for the JJA mean precipitation over (a) the Asian monsoon region and (b) East Asia.

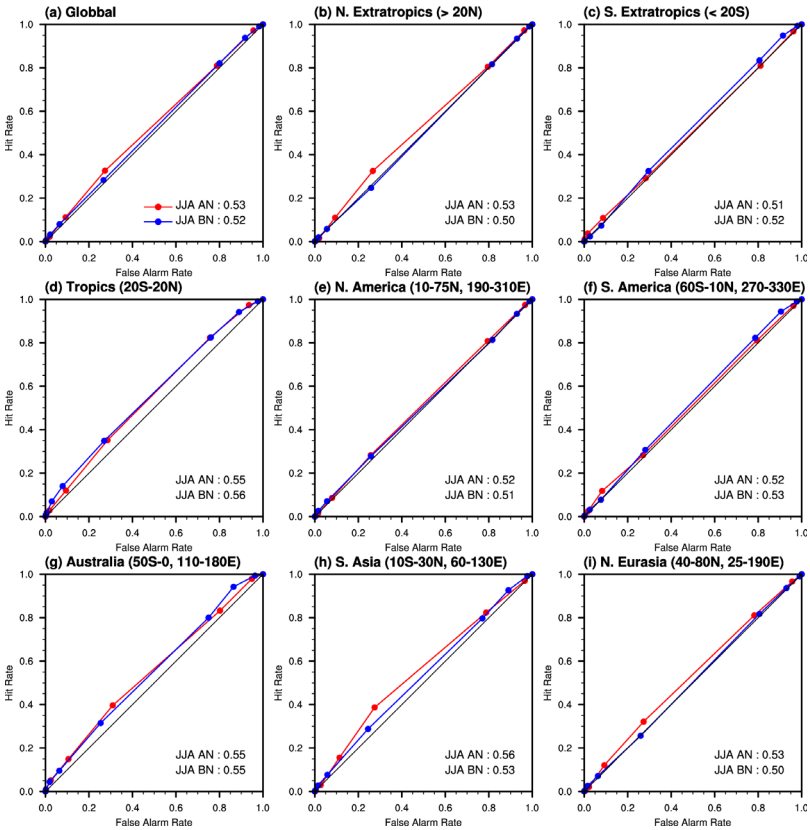

Figure 16 ROC curves for the statistical model for the JJA mean precipitation over the various regions.

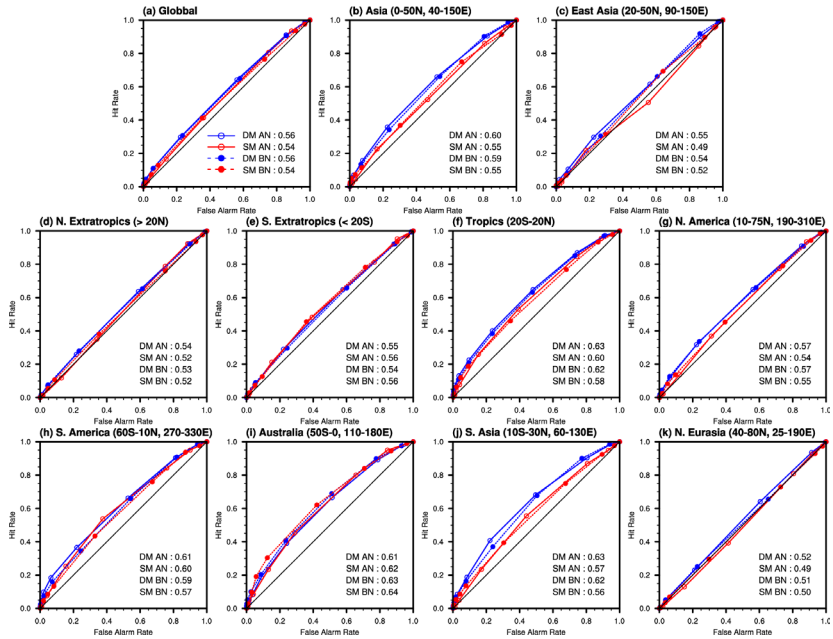

Figure 17 Same as Figure 16 but for the SON mean precipitation over the various regions.

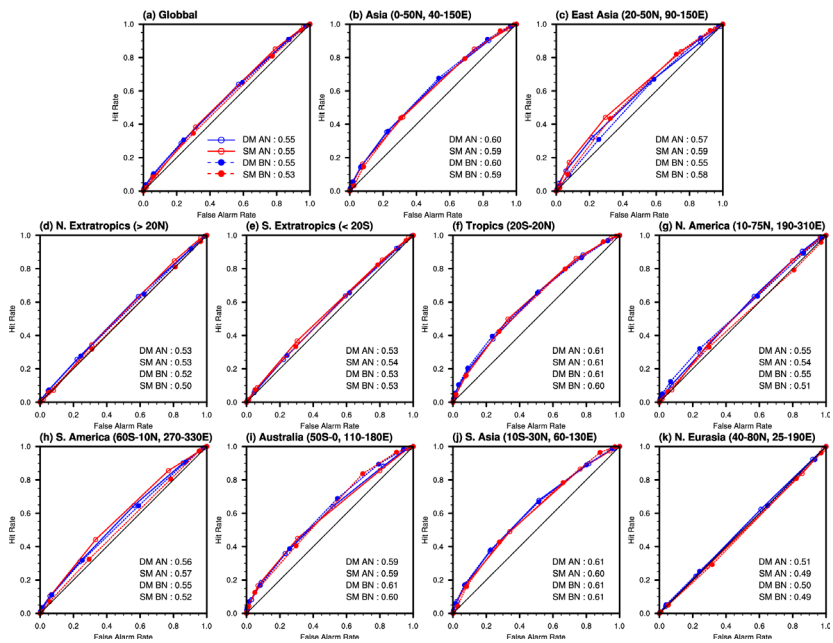

Figure 18 Same as Figure 16 but for the DIF mean precipitation over the various regions.

We also considered alone the inland Asian monsoon and East Asian regions (shown in Figure 19). The difference between the skills achieved for the whole area and those determined for inland areas is most distinct with the statistical model, although the difference in skills is readily apparent over East Asia for both the dynamical and statistical models. Nonetheless, the skills of statistical model are much improved compared with those of the dynamical model for the region. The ENSO originated from the far ocean has considerable impact on the inland region of East Asia, albeit somewhat delayed. The results for the SON and DJF seasons are presented in Figures 20 and 21.

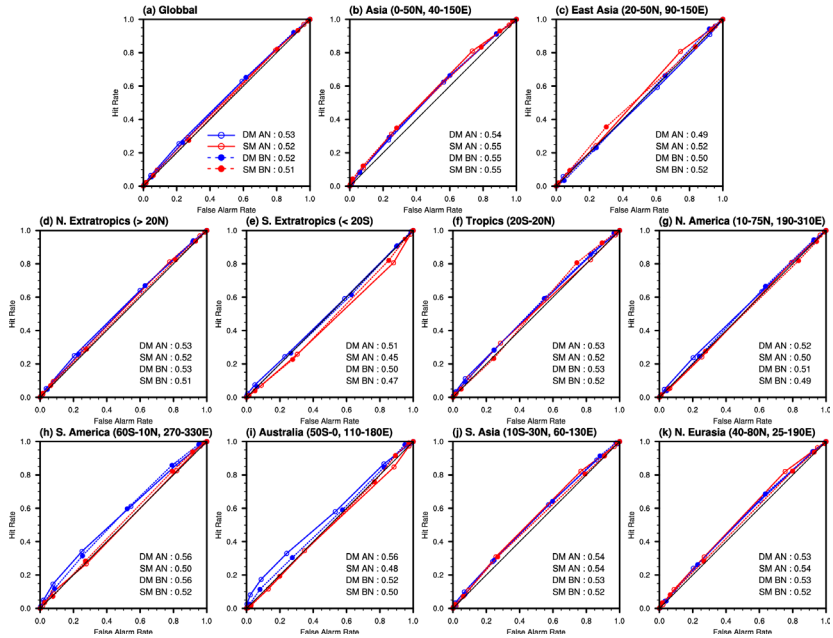

Figure 19 ROC curves of PMMP and the statistical model for the JJA mean precipitation for the various inland regions.

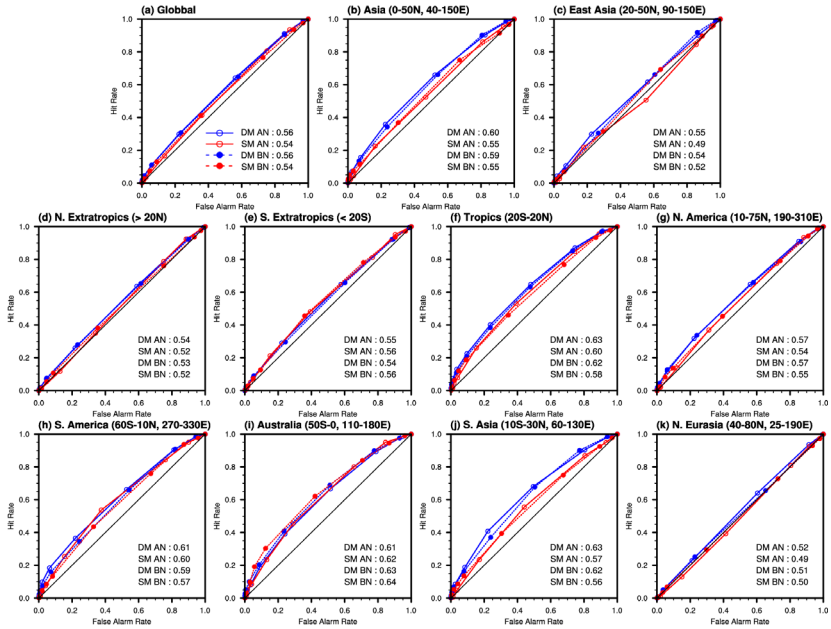

Figure 20 ROC curves of PMMP and the statistical model for the SON mean precipitation for the various inland regions.

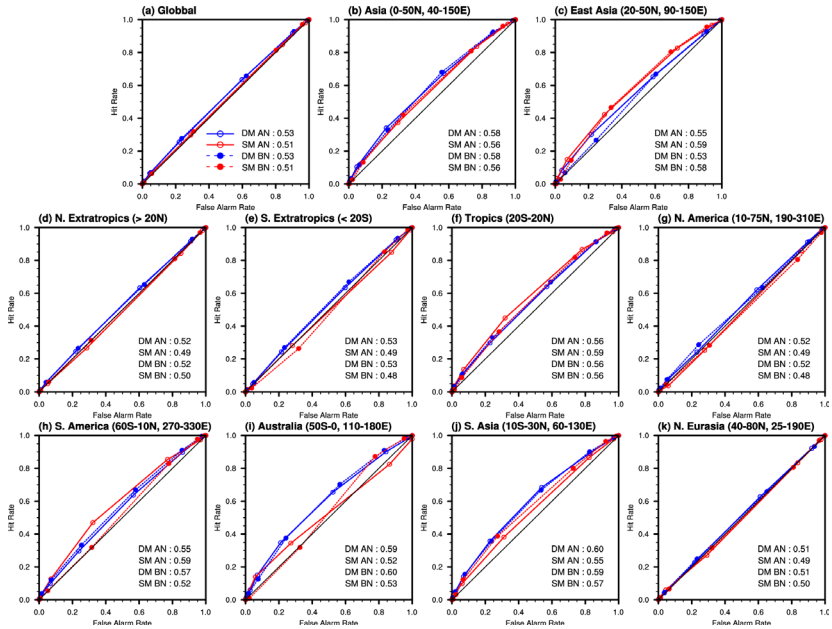

Figure 21 ROC curves of PMMP and the statistical model for the DJF mean precipitation for the various inland regions.

In general, the statistical model outperforms PMMP during the hindcast period of 1983 to 2005. However, its superior skill can still be related to overfitting, even though cross validation is being used to assess the statistical model. Next, we will examine the real-time PMMP and independent statistical prediction for the ASM precipitation during the five year period of 2006-2010.

3.4 Dynamical versus statistical prediction

This section compares PMMP and the statistical model during the hindcast and real-time forecast periods. Since the real-time coupled MME prediction has been operational for only a few years, there is not a sufficient number of samples to obtain quantitative estimates and make a well-grounded conclusion. Nonetheless, it is still worthwhile to examine the recent real-time operational forecasts. We will first show case studies for two summers after the mature phase of El Niño (1998 and 2010) and two summers after the mature phase of La Niña (1999 and 2009) (see Figure 22).

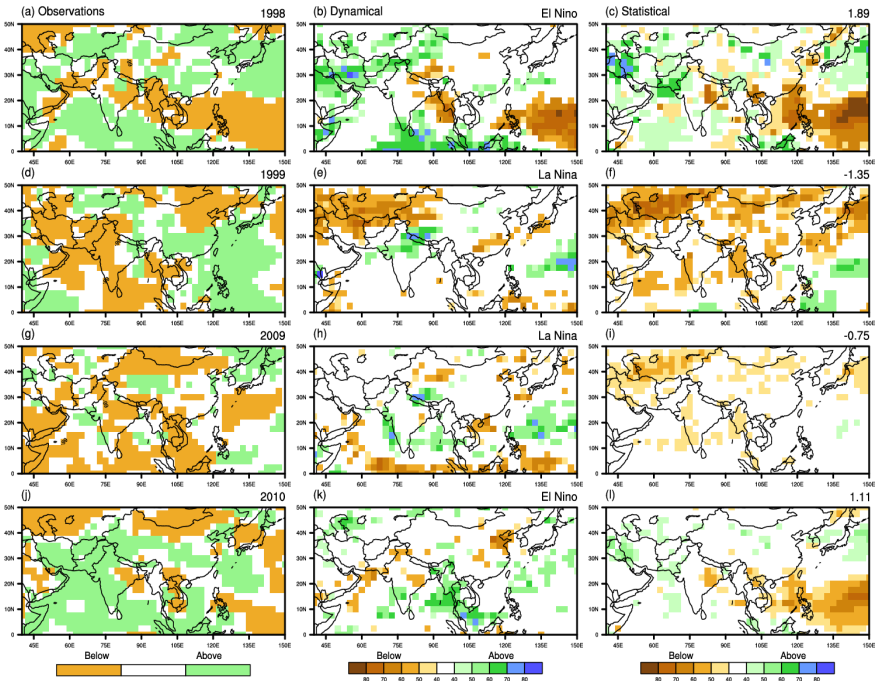

Figure 22 Anomalous JJA mean precipitation from (a, d, g, j) observations, and probabilities (%) from (b, e, h, k) PMMP, and (c, f, i, l) the statistical model for the years 1998 and 1999 (hindcast), and for 2009 and 2010 (real-time forecast). Probabilities for both the AN and BN categories are shown in the same map as is PMMP and the statistical model predictions. Standardized Nino 3.4 indices for the preceding DJF seasons are provided in the upper right of the right panels.

The two summers after the mature phase of El Niño selected here exhibit quite different precipitation anomalies in observations, particularly over East Asia. The summer of 1998 shows the typical impact pattern of a decaying El Niño, with wetter-than-normal conditions over East Asia, parts of the Indian continent and the Indian Ocean, and drier-than-normal conditions over the Bay of Bengal, South China Sea, the Philippine Sea, and the tropical Western Pacific. Whereas the 1998 summer has a dipole pattern of anomalous precipitation over the tropical Western Pacific and East Asia (WP-EA), the 2010 summer has triple pattern over the region of interest. It has been suggested that the 2009/10 event might be an atypical El Niño, i.e. El Niño Modoki [Ashok et al., 2007] or Central-Pacific type El Niño [Yu and Kao, 2007; Kao and Yu, 2009], which yields different patterns of sea-surface warming and cooling in the tropical Pacific and impacts the extratropical region differently

than the typical El Niño. It is interesting to note that PMMP has better skill than the statistical model for the 2010 summer, while the statistical model is more skillful for the summer of 1998. Apparently, the statistical model is unable to capture the impact of an atypical ENSO on the precipitation over the WP-EA region.

The above cases for the two summers after the mature phase of La Niña indicate that the current statistical model is more useful for predicting the below-normal precipitation conditions over many parts of Asia. In the 1999 summer, below-normal conditions were found over continental Asia (except southern China) and above-normal conditions were seen over the Philippines and the surrounding area. In the statistical prediction, La Niña is shown to have great impact on the drier-than-normal conditions over continental Asia, and the dry signals over part of Western Asia, Mongolia, and northeast China are consistent with observations. PMMP, however, predicts below normal rainfall only over part of Western Asia, and near normal or uncertain rainfall over most of continental Asia. The observed pattern of the 2009 summer is similar to that of 1999, that is, below normal conditions over most of continental Asia save for western China. Since the magnitudes of the Niño 3.4 indices for 1998/99 and 2008/09 are different, the strengths of impacts associated with the La Niña events given by the statistical models are also different. In other words, the patterns of the statistical model are consistent, but the strengths of the associated patterns are different. However, PMMP indicated that most of the Asia monsoon region would be near normal or uncertain. Results for the rest of the real-time forecasts are shown in Figure 23.

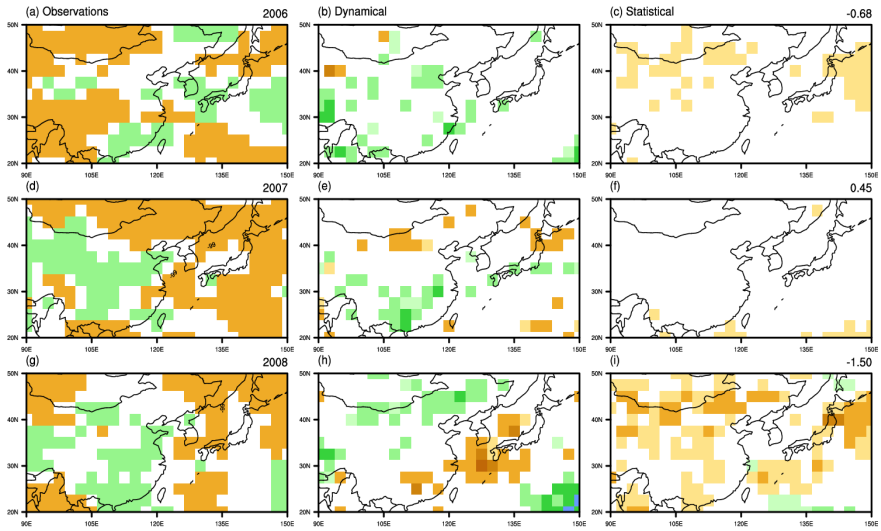

Figure 23 Anomalous JJA mean precipitation from (a, d, g) observations, and probabilities (%) from (b, e, h) PMMP and (c, f, i) the statistical model for the years 2006 to 2008.

The probabilistic retrospective and real-time seasonal forecasts are assessed together for the ASM and East Asian regions. In general, the regionally aggregated skill of the statistical model for the Asia monsoon region is higher than that of the dynamical model during the hindcast period (shown in Figure 24). The skills of the real-time forecasts for both models are within the range of the interannual variability of the historical forecast and are comparable to each other.

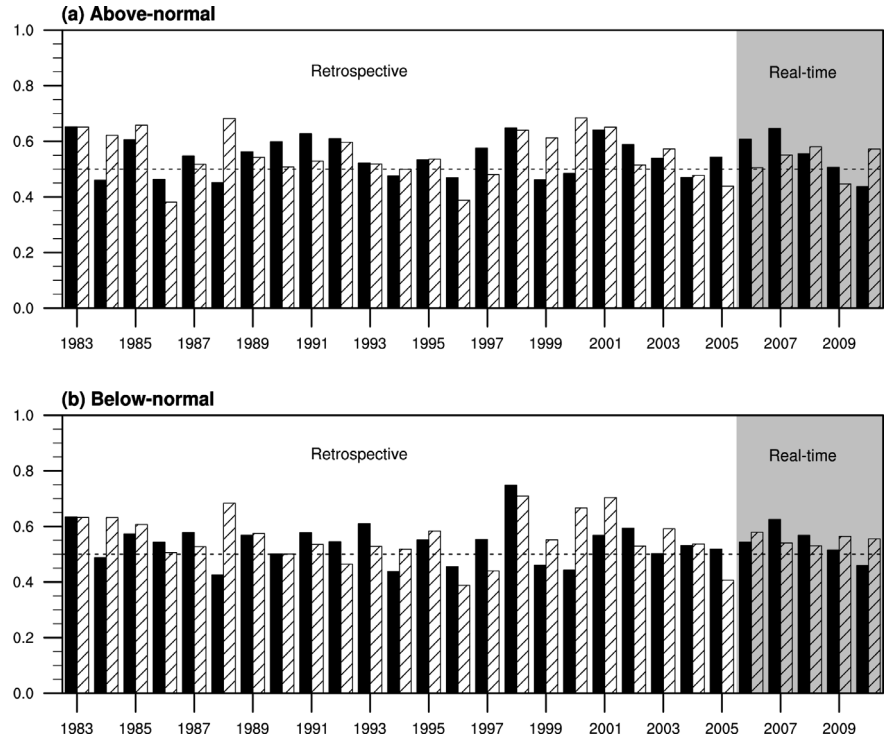

Figure 24 ROCS of historical (1983-2005) and real-time (2006-2010) JJA mean precipitation predictions for the (a) AN and (b) BN categories for the ASM region. Solid bars denote PMMP and hatched bars denote statistical model forecasts.

Figure 25 summarizes the skill comparison between PMMP and the statistical model for both the hindcast (or cross-validated) period (1983-2005) and the real-time (or independent) period (2006-2010). First, it can be seen that the statistical model generally has better skill for the JJA precipitation over the East Asian region for both the AN and BN categories than does PMMP during the hindcast period. However, PMMP is found to be more skillful after the mature phase of atypical ENSO events such as those occurring during the summers of 1992, 2003, and 2005. Second, PMMP also seems to have better skill than the statistical predictions during the independent forecast period of 2006 to 2010, suggesting that cross-validation may still overestimate the forecast skill of the statistical model. Finally, it is notable that the PMM prediction skill is substantially better the averaged skill of all individual coupled models when the skill of the PMM prediction is higher than 0.5 (shown in Figures 26 and 27).

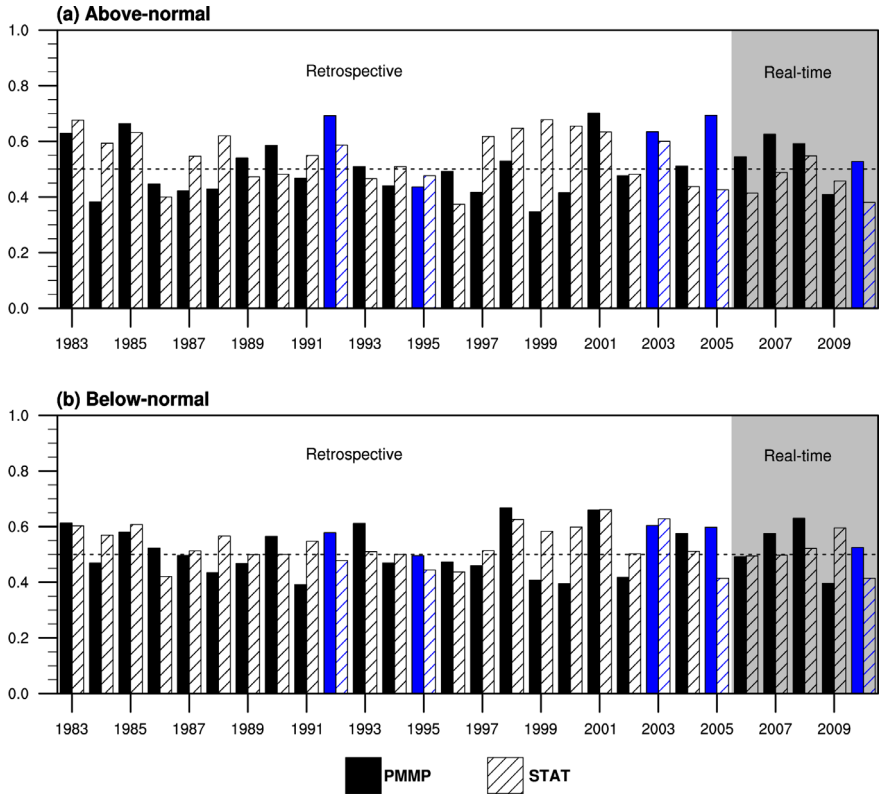

Figure 25 ROCS of historical (1983-2005) and real-time (2006-2010) JJA mean precipitation predictions for the (a) AN and (b) BN categories for East Asia. Solid bars denote PMMP and hatched bars denote statistical model forecasts. Blue bars indicate the summers after the peak of El Niño Modoki events.

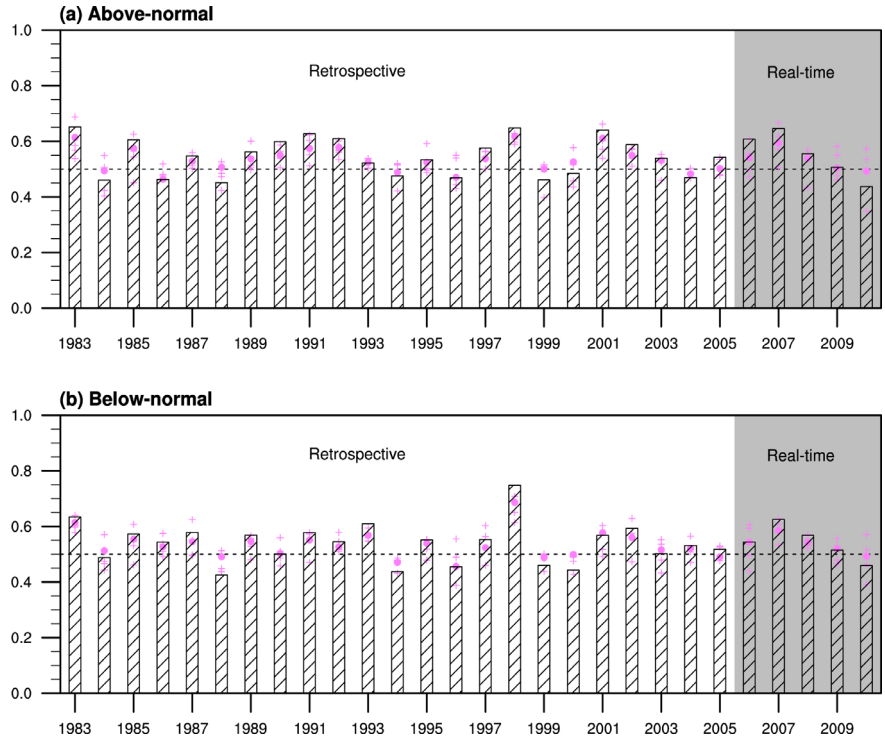

Figure 26 ROCS of PMMP for historical (1983-2005) and real-time (2006-2010) JJA mean precipitation for the (a) AN and (b) BN categories for the ASM region. Hatched bars denote PMMP, and crosses and closed circles indicate individual model forecasts and their simple averages, respectively.

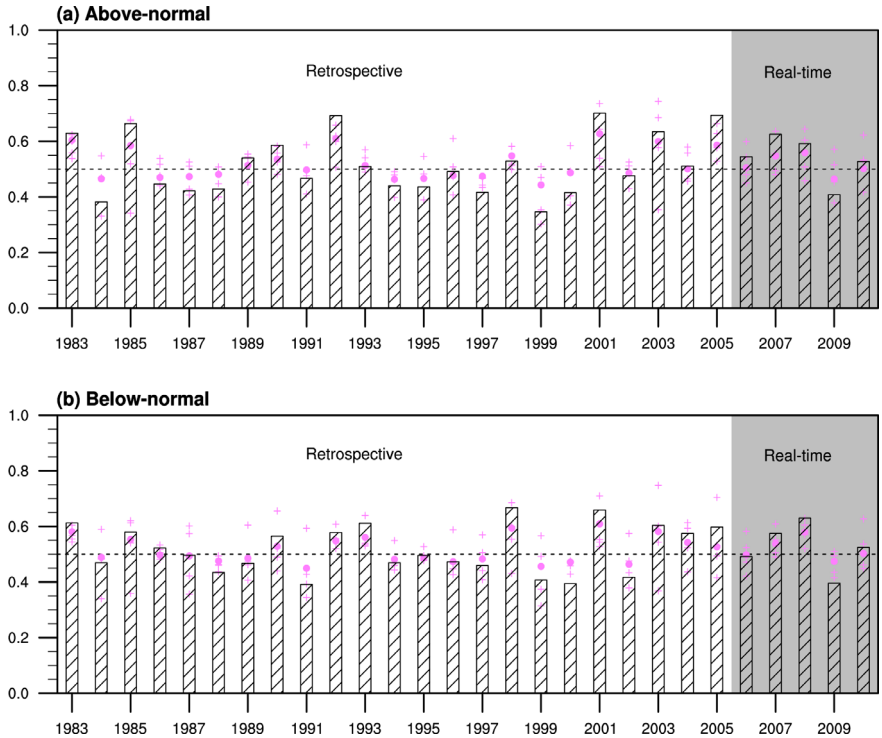

Figure 27 ROCS of PMMP for historical (1983-2005) and real-time (2006-2010) JJA mean precipitation for the (a) AN and (b) BN categories for East Asia. Hatched bars denote PMMP, and crosses and closed circles indicate individual model forecasts and their simple averages, respectively.

The dependency of the forecast skills on the ENSO phase is further investigated. Tables 2 and 3 give a summary of the PMMP and statistical model forecast skills during the summers after the mature phase of El Niño, La Niña and after normal winters. First, the statistical forecast is more sensitive to the ENSO phase than is PMMP. The statistical model has the highest skill during summers after the mature phase of El Niño but the lowest skill during summers after normal winters over both the ASM and East Asian regions. Second, PMMP exhibits the lowest skill during summers after the mature phase of La Niña over the ASM and East Asian regions. During neutral years, PMMP has better skill than the statistical model, while the statistical model performs better during summers after El Niño or La Niña. Results in this study suggest that the statistical model has the potential to improve long-lead predictions of ASM precipitation. On the other hand, it is also clear that PMMP performs

better in summers after normal or atypical ENSO winters.

Table 2 ROCS of PMMP and statistical JJA mean precipitation forecasts for the ASM region for the AN and BN categories, for the period covering both historical and real-time forecasts. Values in brackets are the ROCS for historical forecasts only.

	AN		BN	
	PMMP	Statistical	PMMP	Statistical
All years	0.55 (0.54)	0.55 (0.55)	0.54 (0.54)	0.56 (0.56)
El Nino years	0.55 (0.57)	0.60 (0.60)	0.56 (0.57)	0.59 (0.60)
Neutral years	0.56 (0.55)	0.50 (0.50)	0.55 (0.54)	0.50 (0.50)
La Nina years	0.53 (0.52)	0.55 (0.57)	0.52 (0.51)	0.57 (0.58)

Table 3 ROCS of PMMP and statistical JJA mean precipitation forecasts for the East Asian region for the AN and BN categories, for the period covering both historical and real-time forecasts. Values in brackets are the ROCS for historical forecasts only.

	AN		BN	
	PMMP	Statistical	PMMP	Statistical
All years	0.52 (0.52)	0.53 (0.55)	0.52 (0.52)	0.53 (0.53)
El Nino years	0.54 (0.54)	0.57 (0.59)	0.55 (0.56)	0.53 (0.55)
Neutral years	0.53 (0.51)	0.50 (0.50)	0.52 (0.51)	0.50 (0.50)
La Nina years	0.50 (0.50)	0.53 (0.55)	0.50 (0.50)	0.54 (0.55)

3.5 JJA 2010 forecast from the statistical model

Figure 28 shows JJA 2010 forecast from the statistical model.

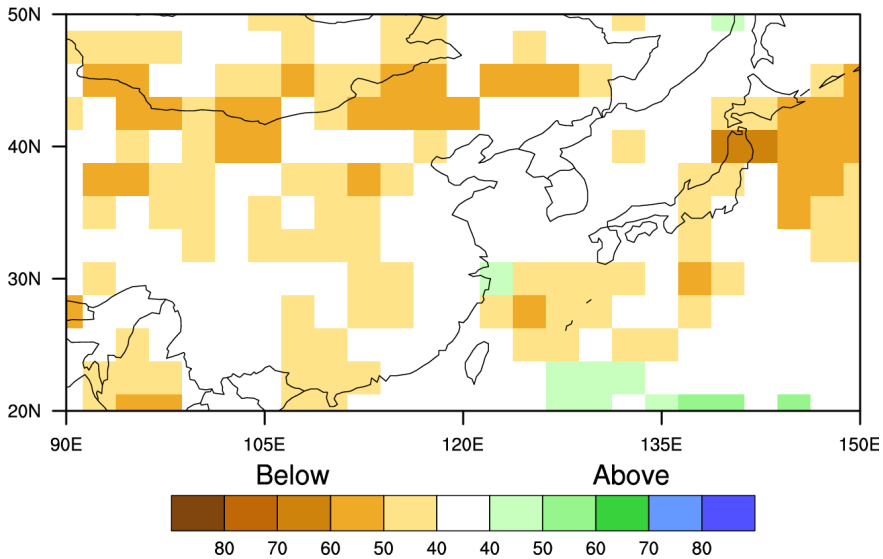

Figure 28 JJA 2010 forecast from the statistical model.

4. DISCUSSION

The long-lead probabilistic predictions with the APCC multi-model system and a statistical model for ASM precipitation, during the period of 1983 to 2010, have been assessed. Particular attention has been paid to the probabilistic prediction of precipitation in summer after the mature phase of ENSO. It is found that the general patterns of prediction skill for the MAM and JJA precipitation are almost the same as those computed for seasons after the mature phase of ENSO. On the other hand, the skill of the MAM forecast is no greater than that for the JJA season after ENSO-neutral winters. This suggests that the skill of the coupled models in predicting the MAM and JJA precipitation mainly comes from their ability to capture the ENSO-related teleconnection.

Previous studies have suggested that the ASM precipitation in summers after the mature phase of ENSO tends to be more predictable than those following ENSO-neutral winters. We have therefore developed a simple lag-regression-based empirical probabilistic forecast model for the ASM precipitation, using the preceding winter ENSO condition as a predictor. The regional distributions of probabilistic composites associated with El Niño and La Niña are not mirror images of each other. After the peak phase of El Niño, the composite patterns related between the distributions indicate wetter-than-normal conditions over the Indian Ocean, Central Asia, the central part of northern China, Northeast Asia, Korea and Japan, and drier-than-normal conditions along coastal East Asia, eastern India and the tropical Western Pacific. After the peak of La Niña, drier-than-normal conditions are more likely to be found in many locations in continental Asia. Recent studies have identified asymmetry in the spatial structures and durations of El Niño and La Niña [*McPhaden and Zhang*, 2009; *Obha et al*., 2010], and such differences might be the cause of the differently lagged impacts.

The comparison of PMMP and the statistical model prediction of the ASM precipitation indicates that, in general, the statistical model outperforms PMMP for the retrospective forecast period, while PMMP is more skillful during the real-time forecast period, for both the AN and BN categories. This could be due to the cross-validated skill of the statistical model being an overestimation of its true skill. The statistical forecast is more sensitive to the ENSO phase, compared to PMMP, and proves to be valuable in capturing the La Niña-related teleconnection. However, the statistical forecast cannot properly capture the atmospheric impact due to atypical ENSO events during the early 1990s and the recent decade. While PMMP exhibits the lowest skill during summers after the mature phase of La Niña, it gives a more stable and consistent forecast skill than the statistical approach, even during atypical ENSO or normal years.

The statistical model should be designed and assessed carefully to avoid artificial predictability since it is highly dependent on limited predictors and the duration of its training period. Because the statistical model adopted here uses the ENSO phase in the preceding boreal winter as a predictor and was trained for only 23

years, it might not be able to capture signals associated with other climate modes or impacts due to the changing background climate. For instance, the East Asian summer monsoon can also be affected by the simultaneous local SST variability [*Lee et al*., 2011b], North Atlantic Oscillation (NAO; *Wu et al*. [2009]), and Eurasian pattern activity [*Lee et al*., 2005, *Min and Jhun*, 2010]. There has also been a decadal change of the East Asia-WNP summer monsoon from an ENSO-related oscillation in 1979-1993 to a monsoon-dominated oscillation in 1994-2004 [*Kwon et al*., 2005]. Moreover, some of the recent Pacific warming events have shown different characteristics compared to the conventional El Niño [*Ashok and Yamagata*, 2009], which leads to different impacts on the East Asian rainfall after the peak of ENSO [*Feng et al*., 2010].

5. CONCLUSION

Finally, it is worthwhile to diagnose the skill of PMMP comprising state-of-the-art coupled models, and to compare it with that of the pure statistical model, focusing on the ASM precipitation after the mature phase of ENSO. The statistical model, which trades off goodness-of-fit against for stability, has the potential to improve long-lead predictions. On the other hand, PMMP is found to be more stable, probably because it is based on direct outputs from dynamical models. Especially, dynamical ENSO prediction skills are reasonably good on long-range time scales up to 6 months and beyond. Therefore, to improve the long-lead ASM precipitation forecast skills, the statistical post-processing of model outputs (e.g. downscaling) can be also applied by utilizing relatively predictable information from dynamical models as the predictor.

REFERENCES

Alessandri, A., A. Borrelli, A. Navarra et al., 2011: Evaluation of probabilistic quality and value of the ENSEMBELS multi-model seasonal forecasts: comparison with DEMETER, Mon. Wea. Rev., doi:10.1175/2010MWR3417.1, in press.

Anderson, J., H. van den Dool, A. G. Barnston, W. Chen, W. Stern, and J. Ploshay, 1999: Present-day capabilities of numerical and statistical models for atmospheric extratropical seasonal simulation and prediction, Bull. Amer. Meteor. Soc., 80(7), 1349-1362.

Ashok, K., S. J, Behara, S. A. Rao, H. Weng, and T. Yamagata, 2007: El Niño Modoki and its possible teleconnection, J. Geophys. Res., 112, C11007, doi:10.1029/2006JC003798.

Ashok, K., and T. Yamagata, 2009: The El Nino with a difference, Nature, 461, 481-484.

Atger, F., 2003: Spatial and interannual variability of the reliability of ensemble-based probabilistic forecasts: Consequences for calibration, Mon. Wea. Rev., 131, 1509-1523.

Atger, F., 2004: Estimation of the reliability of ensemble based probabilistic forecasts, Q. J. R. Meteorol. Soc., 130, 627-646.

Barnston, A. G., M. H. Glantz, and Y. He, 1999: Predictive skill of statistical and dynamical climate models in SST forecasts during the 1997-98 El Nino episode and the 1998 La Nino onset, Bull. Amer. Meteor. Soc., 80, 217-243.

Chowdary, J., S. P. Xie, J. Y. Lee, Y. Kosak, and B. Wang, 2010: Predictability of summer Northwest Pacific climate in eleven coupled model hindcasts: local and remote forcing, J. Geophys. Res., 115, D22121, doi:10.1029/2010JD014595.

Doblas-Reyes, F. J., M. Deque, J. P. Piedelievre, 2000: Multi-model spread and probabilistic seasonal forecasts in PROVOST, Q. J. R. Meteorol. Soc., 126, 2069-2088.

Graham, R. J., M. Gordon, P. J. McLean et al., 2005: A performance comparison of coupled and uncoupled versions of the Met Office seasonal prediction general circulation model, Tellus, 320-339.

Green, D. M., and J. A. Swets, 1966: Signal detection theory and psychophysics, Wiley, New York.

Feng, J., W. Chen, C. Y. Tam, and W. Zhou, 2010: Different impacts of El Niño and El Niño Modoki on China rainfall in the decaying phases, Int. J. Climatol., doi:10.1002/joc.2217.

Ham, Y. G., and I. S. Kang, 2010: Improvement of seasonal forecasts with inclusion of tropical instability waves on initial conditions, Clim. Dyn., doi:10.1007/s00382-010-0743-0.

Janowiak, J. E., and P. Xie, 1999: CAMS_OPI: a global satellite-rain gauge merged product for real-time precipitation monitoring applications, J. Clim., 12, 3335-3342.

Jeong, H. I. et al., 2008: Experimental 6-month hindcast and forecast simulation using CCSM3, APCC 2008 Tech. Rep., APEC Climate Center

Jin, E. K., J. L. III Kinter, B. Wang, C. K. Park, I. S. Kang, B. P. Kitman, J. S. Kug, A. Kumar, J. J. Luo, J. Schemm, J. Shukla, and T. Yamagata, 2008: Current status of ENSO prediction skill in coupled ocean-atmosphere models, Clim Dyn., 31, 647-664, doi:10.1007/s00382-008-0397-3.

Jolliffe, I. T., and D. B. Stephenson, 2003: Forecast Verification, John Wiley and Sons.

Kang, I. S., J. Y. Lee, and C. K. Park, 2004: Potential predictability of summer mean precipitation in a dynamical seasonal prediction system with systematic error correction, J. Clim., 17, 834-844.

Kao, H. Y., and J. Y. Yu, 2009: Contrasting eastern-Pacific and central-Pacific types of ENSO, J. Clim., 22, 615-631, doi:10.1175/2008JCLI2309.1.

Kug, J. S., J. Y. Lee, I. S. Kang, B. Wang, and C. K. Park, 2008: Optimal multi-model ensemble method in seasonal climate prediction, Asia-Pacific J. Atmos. Sci., 44, 259-267.

Krishnamurti, T. N., C. M. Kishtawal, Z. Zhang et al., 1999: Improved weather and seasonal climate forecasts from multi-model superensemble, Science, 285, 1548-1550, doi:10.1126/science.285.5433.1548.

Krishnamurti, T. N., C. M. Kishtawal, D. W. Shin, and C. E. Williford, 2000: Multi-model superensemble forecasts for weather and seasonal climate, J. Clim., 13, 4196-4216.

Krzysztofowicz, R., 1983, Why should a forecaster and a decision maker use Bayes theorem, Water Resour. Res., 19, 327-336.

Kwon, M. H., J. G. Jhun, B. Wang, S. I. An, and J. S. Kug, 2005: Decadal change in relationship between east Asian and WNP summer monsoon, Geophys. Res. Lett., 32, L16709, doi:10.1029/2005GL023026.

Lee, E. J., J. G. Jhun, and C. K. Park, 2005: Remote connection of the northeast Asian summer rainfall variation reveled by a newly defined monsoon index, J. Clim., 18, 4381-4393.

Lee, J. Y., B. Wang, I. S. Kang, J. Shukla, A. Kumar, J. S. Kug, J. K. E. Schemm, J. J. Luo, T. Yamagata, X. Fu, O. Alves, B. Stern, T. Rosati, and C. K. Park, 2010: How are seasonal prediction skills related to models' performance on mean state and annual cycle?, Clim. Dyn., 35, 267-283, doi:10.1007/s00382-010-0857-4.

Lee, J. Y., B. Wang, Q. Ding, K. J. Ha, J. B. Ahn, A. Kumar, B. Stern, and O. Alves, 2011a: How predictable is the Northern Hemisphere summer upper-tropospheric circulation?, Clim. Dyn., doi:10.1007/s00382-010-0909-9 (In press).

Lee, S. S., J. Y. Lee, K. J. Ha, B. Wang, and J. K. E. Schemm, 2011b: Deficiencies and possibilities for long-lead coupled climate prediction of the Western North Pacific-East Asian summer monsoon, Clim. Dyn., 36, 1173-1188, doi:10.1007/s00382-010-0832-0.

Lee, W. J. et al., 2009: APEC Climate Center for climate information services, APCC 2009 Final Rep. (available at http://www.apcc21.net/en/activities/publications/reports/).

Latif, M. et al., 2001: ENSIP: The El Nino simulation intercomparison project, Clim. Dyn., 18, 255-276.

Liang, J., S. Yang, Z. Z. Hu, B. Huang, A. Kumar, and Z. Zhang, 2009: Predictable patterns of the Asian and Indo-Pacific summer precipitation in the NCEP CFS, Clim. Dyn., 32, 989-1001.

Luo, J. J. et al., 2005: Seasonal climate predictability in a coupled OAGCM using a different approach for ensemble forecasts, J. Clim., 18, 4474-4497.

Mason, I., 1982: A model for assessment of weather forecast, Aust. Meteor. Mag., 30, 291-303.

Mason, S. J., and N. E. Graham, 1999: Conditional probabilities, relative operating characteristics, and relative operating level, Wea. Forecasting, 14, 713-725.

McPhaden, M, J. and X. Zhang, 2009: Asymmetry in zonal phase propagation of ENSO sea surface temperature anomalies. Geophys Res Lett 36. L13703. doi:10.1029/2009GL 038774.

Michaelsen, J., 1987: Cross-validation in statistical forecast model. J. Climate Appl. Meteor 26, 1589-1600.

Min, H. J., and J. G. Jhun, 2010: The change in the East Asian summer monsoon simulated by the MIROC3.2 high-resolution coupled model under global warming scenarios, Asia-Pacific J. Atmos.

Sci., 46, 73-88.

Min, Y. M., V. N. Kryjov, and C. K. Park, 2009: A probabilistic multimodel ensemble approach to seasonal prediction, Wea. Forecasting, 24, 812-828, doi:10.1175/2008WAF2222140.1.

Min, Y. M., J. Y. Lee, J. S. Kug, B. Wang et al., 2011: Improvement of the APCC probabilistic multi-model seasonal prediction by systematic error correction and uncertainty estimation. Submitted to Clim. Dyn.

Moorthi, S., H. L. Pan, and P. Caplan, 2001: Changes to the 2001 NCEP operational MRF/AVN global analysis/forecast system. NWS Technical Procedures Bulletin 484, 14 pp. [Available online at http://www.nws.noaa.gov/om/tpb/484.htm.]

Murphy, A. H., 1973: A new vector partition of the probability score, J. Appl. Meteor., 12, 595-600.

Murphy, A. H., 1977: The value of climatological, categorical, and probabilistic forecasts in the cost-loss ration situation, Mon. Wea. Rev., 105, 803-816.

Murphy, A. H., and R. L. Winkler, 1977: Reliability of subjective probability forecasts of precipitation and temperatures, Appl. Stat., 26, 61-78.

Murphy, A. H., and R. L. Winkler, 1987: A general framework of forecast verification, Mon. Wea. Rev., 115, 1330-1338.

NOAA Climate Test Bed, MME White Paper, 2006 available at http://www.cpc.noaa.gov/products/ctb/ctb-publications.shtml.

Ohba, M, D. Nohara, and H. Ueda, 2010: Simulation of asymmetric ENSO transition in WCRP CMIP3 multi-model experiments. J. Clim., 23(22), 6051-6067, doi: 10.1175/2010JCLI3608.1

Pacanowski, R. C., and S. M. Griffies, cited 1998: MOM 3.0 manual, NOAA/GFDL. [Available online at http://www.gfdl.noaa.gov/~smg/MOM/web/guide_parent/guide_parent.html.]

Palmer, T. N., C. Brankovic, and D. S. Richardson, 2000: A probability and decision-model analysis of PROBOST seasonal multi-model ensemble integrations, Q. J. R. Meteorol. Soc., 126, 2013-2034.

Palmer, T. N., A. Alessandri, U. Andersen et al., 2004: Development of a European multi-model ensemble system for seasonal to inter-annual prediction, Bull. Amer. Meteor. Soc., 85, 853-872.

Reynolds, R. W., N. A. Rayner, T. M. Smith, D. C. Stokes, and W. Wang, 2002: An improved in situ and satellite SST analysis for climate, J. Clim., 15, 1609-1625.

Richardson, D. S., 2000: Skill and economic value of the ECMWF ensemble prediction system, Q. J. R. Meteorol. Soc., 126, 649-668, doi:10.1002/qj.49712656313.

Richardson, D., 2006: Predictability and economic value, in Predictability of Weather and Climate, edited by T. Palmer, and R. Hagedorn, pp. 628—644, Cambridge Univ. Press.

Roeckner, E., and Coauthors, 1996: The atmospheric general circulation model ECHAM-4: Model description and simulation of present-day climate. Rep. 218, Max-Plank Institut fur Meteorologie, Hamburg, Germany, 90 pp. [Available from MPI, Bundestrasse 55, Hamburg, D-20146 Germany.]

Saha, S., S. Nadiga, C. Thiaw et al., 2006: The NCEP Climate Forecast System, J. Clim., 19, 3483-3517.

Shukla, J. et al., 2000: Dynamical seasonal prediction, Bull. Am. Meteorol. Soc., 81, 2493-2606, doi:10.1175/1520-0477(2000)081〈2593:DSP〉2.3.CO;2.

Sohn, S. J., C. Y. Tam, K. Ashok, and J. B. Ahn, 2011: Quantifying the reliability of precipitation datasets for monitoring large-scale East Asian precipitation variations, Int. J. Climatol. (Accepted).

Stanski, H., L. Wilson, and W. Burrows, 1989: Survey of common verification methods in meteorology, Tech. Rep. WMO/TD No. 358, WMO World Weather Watch.

Stephenson, D. B., and F. J. Doblas-Reyes, 2000: Statistical methods for interpreting Monte Carlo ensemble forecasts, Tellus, 52A, 300-322.

Swets, J. A., 1973: The relative operating characteristics in psychology, Science, 182, 990-1000.

Tracton, M. S., and E. Kalnay, 1993: Operational ensemble prediction at the National Meteorological Center: Practical aspects, Wea. Forecasting, 8, 379–398.

van Oldenborgh, G. J., M. A. Balmaseda, L, Ferranti, T. N. Stockdale, and D. L. T Anderson, 2005: Did the ECMWF seasonal forecast model outperform statistical ENSO forecast models over the Last 15 years?, J. Clim., 18, 3240-3249.

Wang, B., I. S. Kang, and J. Y. Lee, 2004: Ensemble simulations of Asian-Australian monsoon variability by 11 AGCMs, J. Clim., 17, 803-818.

Wang, B., J. Y. Lee, I. S. Kang, J. Shukla, N. H. Saji, and C. K. Park, 2007: Coupled predictability of seasonal tropical precipitation, CLIVAR Exchanges, 12, 17-18.

Wang, B., J. Y. Lee, I. S, Kang, J. Shukla et al., 2008: How accurately do coupled climate models predict the Asian-Australian monsoon interannual variability?, Clim. Dyn., 30, 605-619, doi:10.1007/s00382-007-0310-5.

Wang, B., Z. Wu, J. Li, J. Liu, C. P. Chang, Y. Ding, and G. Wu, 2008: How to measure the strength of the east Asian summer monsoon?, J. Clim., 21, 4449-4463, doi:10.1175/2008JCLI2183.1.

Wang, B., J. Y. Lee, I. S. Kang, J. Shukla, C. K. Park et al., 2009: Advance and prospectus of seasonal prediction: Assessment of the APCC/CliPAS 14-model ensemble retrospective seasonal prediction (1980-2004), Clim. Dyn., 33, 93-117, doi: 10.1007/s00382-008-0460-0.

Wilks, D. S., 1995: Statistical Methods in the Atmospheric Sciences: An Introduction, Academic Press.

WMO, 2002: Standardised Verification System (SVS) for Long-Range Forecasts (LRF), New attachment II-9 to the manual on the GDPS, Vol. 1. WMO-No. 485, 24 pp.

Wu, Z., B. Wang, J. Li, and F. F. Jin, 2009: An empirical seasonal prediction model of the east Asian summer monsoon using ENSO and NAO, J. Geophys. Res., 114, D18120, doi:10.1029/2009JD011733.

Yu, J. Y., and H. K. Kao, 2007: Decadal changes of ENSO persistence barrier in SST and ocean heat content indices: 1958-2001, J. Geophys. Res., 112, D13106, doi:10.1029/2006JD007654.

Zhu, Y., Z. Toth, R. Wobus, D. Richardson, and K. Mylne, 2002: The economic value of ensemble-based weather forecasts, Bull. Am. Meteorol. Soc., 83, 73-83, doi:10.1175/1520-0477(2002)083〈0072:TEVOEB〉2.3.CO;2.

APCC TECHNICAL REPORT 2011-02

- Improvement of MME Seasonal Prediction Skill
- Assessment of the Long-Lead Probabilistic Prediction
- Improvement of the APCC Probabilistic Multi-Model Ensemble Prediction

APEC Climate Center

12, Centum 7-ro, Haeundae-gu, Busan 612-020,
Republic of Korea
Tel: +82-51-745-3900 Fax: +82-51-745-3949
www.apcc21.org

비매품
94500
9 788997 533172
ISBN 978-89-97333-17-2
ISBN 978-89-97333-15-8 (세트)